Structure–function analysis and genetic interactions of the SmG, SmE, and SmF subunits of the yeast Sm protein ring

BEATE SCHWER,[1] JOSHUA KRUCHTEN,[1] and STEWART SHUMAN[2]

[1]Microbiology and Immunology Department, Weill Cornell Medical College, New York, New York 10065, USA
[2]Molecular Biology Program, Sloan-Kettering Institute, New York, New York 10065, USA

ABSTRACT

A seven-subunit Sm protein ring forms a core scaffold of the U1, U2, U4, and U5 snRNPs that direct pre-mRNA splicing. Using human snRNP structures to guide mutagenesis in *Saccharomyces cerevisiae*, we gained new insights into structure–function relationships of the SmG, SmE, and SmF subunits. An alanine scan of 19 conserved amino acids of these three proteins, comprising the Sm RNA binding sites or inter-subunit interfaces, revealed that, with the exception of Arg74 in SmF, none are essential for yeast growth. Yet, for SmG, SmE, and SmF, as for many components of the yeast spliceosome, the effects of perturbing protein–RNA and protein–protein interactions are masked by built-in functional redundancies of the splicing machine. For example, tests for genetic interactions with non-Sm splicing factors showed that many benign mutations of SmG, SmE, and SmF (and of SmB and SmD3) were synthetically lethal with null alleles of U2 snRNP subunits Lea1 and Msl1. Tests of pairwise combinations of SmG, SmE, SmF, SmB, and SmD3 alleles highlighted the inherent redundancies within the Sm ring, whereby simultaneous mutations of the RNA binding sites of any two of the Sm subunits are lethal. Our results suggest that six intact RNA binding sites in the Sm ring suffice for function but five sites may not.

Keywords: Sm ring subunits; pre-mRNA splicing; snRNPs

INTRODUCTION

Seven different Sm proteins (B, D1, D2, D3, E, F, and G) assemble into a toroidal ring that forms the core scaffold of the U1, U2, U4, and U5 small ribonuclear proteins (snRNPs) that orchestrate pre-mRNA splicing (van der Feltz et al. 2012; Kondo et al. 2015; Li et al. 2016). The conserved fold of each Sm subunit comprises a five-strand antiparallel β sheet of topology β5↑•β1↓•β2↑•β3↓•β4↑ (shown for SmG in Fig. 1A). Several of the Sm subunits are embellished by additional secondary structure elements and/or unstructured C-terminal extensions of varying length. Prior to assembly of the ring, the Sm subunits self-organize as three heteromeric subcomplexes: D3–B, F–E–G, and D1–D2 (Kambach et al. 1999). The assembled Sm ring is stabilized by main-chain and side-chain contacts between neighboring Sm subunits and by interactions with the uridine-rich Sm site of the snRNA, which threads through the central hole of the Sm ring so that the individual RNA nucleobases are engaged sequentially by the SmF, SmE, SmG, SmD3, SmB, SmD1, and SmD2 subunits (Kondo et al. 2015; Li et al. 2016). This entails a stereotypic set of Sm protein–RNA contacts by an amino acid "triad" whereby the planar nucleobase is sandwiched by an arginine or lysine side chain from the β4–β5 loop (which makes a π-cation stack on the nucleobase) and a side chain from the β2–β3 loop (often an aromatic group that forms a π stack on the nucleobase), while an asparagine side chain of the β2–β3 loop makes hydrogen bonds to the nucleobase edge (Fig. 1A).

The assembly of the human Sm ring around the Sm RNA site is an intricate and ordered process mediated by the SMN complex, comprising the SMN (survival motor neuron) protein and several Gemin proteins, and other factors (Liu et al. 1997; Zhang et al. 2011; Grimm et al. 2013; Neuenkirchen et al. 2015). Mutations in the human *SMN1* gene are the cause of the disease spinal muscular atrophy (Lunn and Wang 2008; Chari et al. 2009). Less is known about the Sm assembly pathway in the simpler model organism *Saccharomyces cerevisiae*, beyond the fact that budding yeast has, in Brr1, a putative homolog of the key metazoan Sm assembly factor Gemin2 (Noble and Guthrie 1996; Liu et al. 1997; Kroiss et al. 2008). Although the structure of the mature human Sm ring and its RNA interface is known (Kambach et al. 1999; Weber et al. 2010; Kondo et al. 2015; Li et al. 2016), and recent cryo-EM studies of splicing complexes are providing

Corresponding authors: bschwer@med.cornell.edu, s-shuman@ski.mskcc.org

Article published online ahead of print. Article and publication date are at http://www.rnajournal.org/cgi/doi/10.1261/rna.057448.116. Freely available online through the *RNA* Open Access option.

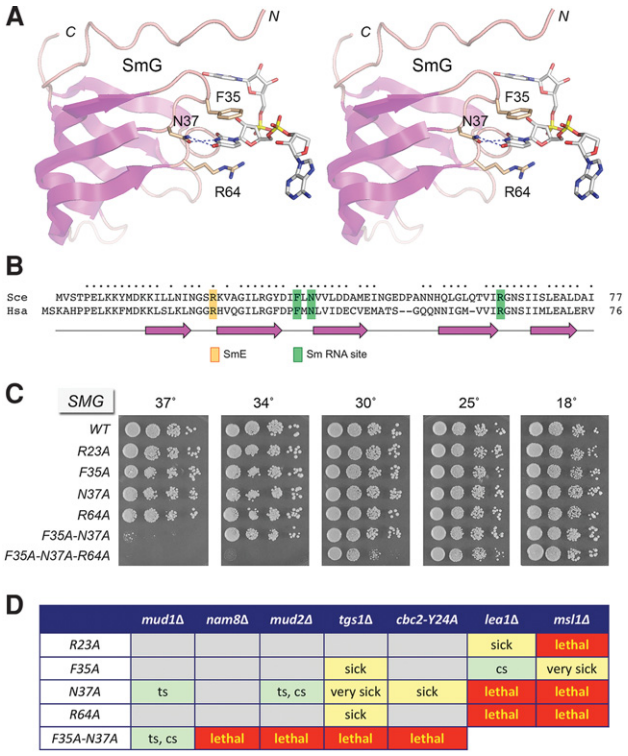

FIGURE 1. Structure-guided mutagenesis of SmG. (*A*) Stereo view of the human U1 snRNP structure highlighting the fold of SmG (depicted as a cartoon trace with magenta β strands) and its interactions with the Sm site in U1 snRNA. Selected amino acids are shown as stick models and numbered according to their positions in the yeast SmG polypeptide. Atomic contacts are indicated by dashed lines. (*B*) Alignment of the primary structures of the *S. cerevisiae* (Sce) and human (Hsa) SmG. Positions of side chain identity/similarity are indicated by (•) *above* the yeast sequence. The secondary structure elements are depicted *below* the human sequence, with β strands as magenta arrows. SmG amino acids that make contacts to SmE or the U1 snRNA are highlighted in color-coded boxes as indicated. (*C*) The wild-type and mutated *SMG* alleles were tested for *smg*Δ complementation by plasmid shuffle. The viable FOA-resistant *smg*Δ strains bearing the indicated *SMG* alleles were spot-tested for growth on YPD agar at the temperatures specified. (*D*) Synthetic interactions of SmG mutants. Synthetically lethal pairs of alleles are highlighted in red boxes. Other negative pairwise interactions are classified as sick or very sick (yellow boxes) or temperature-sensitive (*ts*) or cold-sensitive (*cs*) (light green boxes). Gray boxes denote lack of mutational synergy.

similar insights into the budding and fission yeast Sm rings (Hang et al. 2015; Nguyen et al. 2015; Wan et al. 2016), there has been scant genetic analysis of the yeast Sm proteins beyond the findings that the SmB, SmD1, SmD2, SmD3, SmE, SmF, and SmG proteins are all essential for vegetative growth; the disordered C-terminal tails of SmB, SmD1, and SmD3 are individually dispensable for vegetative growth; and simultaneous deletion of the tails of SmB and SmD1 is synthetically lethal (Bordonné 2000; Zhang et al. 2001).

We recently initiated a structure-guided in vivo mutational analysis of the budding yeast Sm protein ring, focusing first on the adjacent SmD3 and SmB subunits and their atomic interactions with RNA and neighboring proteins (Schwer and Shuman 2015). Our results indicated that none of the SmD3 and SmB amino acids that mediate these contacts are essential per se. However, we defined a network of genetically redundant constituents of SmD3 and SmB that displayed diverse mutational synergies—within the particular Sm subunit, between neighboring subunits of the Sm ring, with U1 snRNP subunits Mud1 and Nam8, with the branch-point-binding protein subunit Mud2, and with the U2 snRNP subunit Lea1.

Alanine scanning of the Sm RNA binding sites of SmD3 (Ser-Asn-Arg) and SmB (His-Asn-Arg) provided new insight into built-in redundancies of the Sm ring, whereby simultaneous mutations of the (individually dispensable) Asn or Arg residues in the adjacent SmD3 and SmB ring subunits were lethal. This suggested that six of seven intact RNA binding sites in the Sm ring can suffice for in vivo function, but five sites may not suffice. Of course, this conclusion applied narrowly to SmD3 and SmB, which comprise a stable heterodimeric subcomplex of the Sm ring. It is conceivable that one or more of the other five Sm protein RNA sites is essential per se, or that yeast might survive if different pairs of RNA sites within the ring were disabled.

Here we addressed these issues via mutational analysis of the RNA sites of the SmG, SmE, and SmF proteins, individually and in various cross-subunit combinations with each other and with SmD3 and SmB mutations. We also surveyed broadly for allele-specific synthetic interactions of SmG, SmE, and SmF with other components of the yeast spliceosome. Our results illustrate how the yeast Sm ring conforms to the apothegm (popularized in song by The Osmonds; www.youtube.com/watch?v=96HqPpjI3UY) that "one bad apple don't spoil the whole bunch."

RESULTS AND DISCUSSION

Structure-guided mutagenesis of yeast SmG

The 77-aa *S. cerevisiae* SmG protein is homologous to the 76-aa human SmG polypeptide, with 55 positions of side chain identity/similarity (Fig. 1B). The fold of human SmG in the U1 snRNP crystal (Kondo et al. 2015) is shown in Figure 1A. The SmG subunit captures a uridine nucleotide of the U1 RNA Sm site. SmG side chain Asn39 (Asn37 in yeast SmG) makes bidentate hydrogen bonds from Nδ and Oδ to the O4 and N3 atoms of the uracil nucleobase (Fig. 1A). SmG Arg63 (Arg64 in yeast SmG) makes the π-cation stack on the uracil. SmG Phe37 (Phe35 in yeast SmG) completes the sandwich on the other face of the uracil (Fig. 1A). SmG Arg25 (Arg23 in yeast SmG) makes bridging hydrogen bonds to the adjacent SmE subunit of the Sm ring. To interrogate the contributions of these contacts, we mutated yeast SmG residues Arg23, Phe35, Asn37, and Arg64 to alanine. The wild-type and *SMG-Ala* alleles were placed on *CEN HIS3* plasmids under the control of the native *SMG* promoter and tested by plasmid shuffle for complementation of a

*smg*Δ p[*CEN URA3 SMG*] strain. The resulting *SMG-Ala* strains were viable after FOA selection and grew as well as wild-type *SMG* cells on YPD agar (Fig. 1C). We conclude that the individual RNA binding side chains are dispensable for yeast SmG function in vivo. To evaluate whether there is functional redundancy of the Sm RNA binding residues of SmG, we constructed a *F35A-N37A* double-mutant and a *F35A-N37A-R64A* triple-mutant. *F35A-N37A* cells grew normally on YPD agar at 18°C–34°C but failed to thrive at 37°C. *F35A-N37A-R64A* cells grew well at 18°C–25°C, slowly at 30°C, and failed to grow 34°C–37°C (Fig. 1C). Thus, compound mutations of the SmG RNA binding site elicited a progressive temperature-sensitive (*ts*) growth defect.

Mutagenesis of yeast SmE

The 94-aa *S. cerevisiae* SmE protein and the 92-aa human SmE polypeptide align with 61 positions of side chain identity/similarity (Fig. 2B). The fold of human SmE in the U1 snRNP crystal (Kondo et al. 2015) is shown in Figure 2A. SmE engages an adenine nucleotide of the U1 RNA Sm site via a Tyr-Asn-Lys triad, the equivalent of which in yeast SmE is Phe49-Asn51-Lys83 (Fig. 2A,B). SmE also contacts a purine base 7 nucleotides (nt) downstream via van der Waals interactions of Tyr36-Glu37, corresponding to Phe32-Glu33 in yeast SmE. SmE amino acids Tyr24 (Phe20 in yeast SmE) and Glu63 (Glu59 in yeast SmE) interact, respectively, with the SmG and SmF subunits that flank SmE within the Sm ring (Fig. 2B). Yeast SmE residues Phe20, Phe32, Glu33, Phe49, Asn51, Glu59, and Lys83 were mutated individually to alanine. The wild-type and *SME-Ala* alleles on *CEN LEU2* plasmids under the control of the native *SME* promoter were tested by plasmid shuffle for complementation of a *sme*Δ p[*CEN URA3 SME*] strain. All seven *SME-Ala* strains were viable after FOA selection and grew as well as wild-type *SME* cells on YPD agar (Fig. 2C). To probe functional redundancy of the SmE RNA binding residues, we tested *F32A-E33A* and *F49A-N51A* double mutants and found that they too grew as well as wild-type cells at all temperatures tested (Fig. 2C). The normal growth of *SME-F49A-N51A* cells is distinguished from the *ts* growth defect of the synonymous *SMG* RNA binding site mutant *F35A-N37A*.

Mutagenesis of yeast SmF

The 86-aa *S. cerevisiae* SmF and human SmF proteins align with 49 positions of side chain identity/similarity (Fig. 3B). The fold of human SmF in the U1 snRNP crystal is shown in Figure 3A. Human SmF binds an adenosine nucleotide of the U1 RNA Sm site via a Tyr39-Asn41-Arg65 triad that corresponds to Tyr48-Asn50-Arg74 in yeast SmF (Fig. 3A, B). Human SmF also contacts a downstream RNA segment via hydrogen bonds to the phosphate–ribose backbone from Lys24 and Arg65 (Lys32 and Arg74 in yeast SmF) and via van der Waals interactions of Lys24-Trp25 (Lys32-

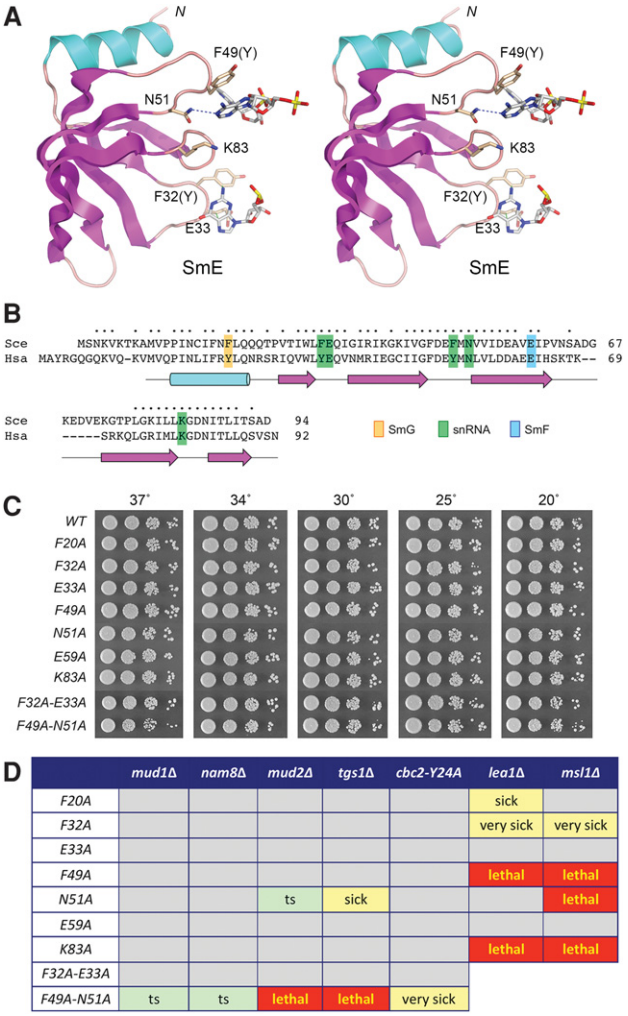

FIGURE 2. Structure-guided mutagenesis of SmE. (*A*) Stereo view of the human U1 snRNP structure highlighting the fold of SmE (depicted as a cartoon trace with magenta β strands and a cyan α helix) and its interactions with the Sm site in U1 snRNA. Selected amino acids are shown as stick models and named and numbered according to their positions in the yeast SmE polypeptide. The counterparts of Phe32 and Phe49 in yeast SmE are tyrosines in human SmE. Atomic contacts are indicated by dashed lines. (*B*) Alignment of the primary structures of the *S. cerevisiae* (Sce) and human (Hsa) SmE. Positions of side chain identity/similarity are indicated by (•) *above* the yeast sequence. The secondary structure elements are depicted *below* the human sequence. SmE amino acids that make contacts to SmG, SmF, or the U1 snRNA are highlighted in color-coded boxes as indicated. (*C*) Wild-type and mutated *SME* alleles were tested for *sme*Δ complementation by plasmid shuffle. The viable FOA-resistant *sme*Δ strains bearing the indicated *SME* alleles were spot-tested for growth on YPD agar at the temperatures specified. (*D*) Synthetic interactions of SmE mutants. Synthetically lethal pairs of alleles are highlighted in red boxes. Other negative pairwise interactions are classified as sick or very sick (yellow boxes) or temperature-sensitive (*ts*) or cold-sensitive (*cs*) (light green boxes). Gray boxes denote lack of mutational synergy.

Phe33 in yeast SmF) with a purine base (Fig. 3A,B). SmF amino acids Asn68 (Asn77 in yeast SmF) and Tyr71 (Tyr80 in yeast SmE) interact, respectively, with flanking SmD2 and SmE subunits (Fig. 3B). SmF Glu49 (equivalent to Glu58

in yeast SmF) contacts the human U1 snRNP subunit U1-70K, the yeast homolog of which is Snp1. Here we mutated yeast SmF residues Lys32, Phe33, Tyr48, Asn50, Glu58, Arg74, Asn77, and Tyr80 individually to alanine. The wild-type and *SMF-Ala* alleles on *CEN LEU2* plasmids under the control of the native *SMF* promoter were tested by plasmid shuffle for complementation of a *smf*Δ p[*CEN URA3 SMF*] strain. All *SMF-Ala* strains except *R74A* grew as well as wild-type *SMF* cells on YPD agar at all temperatures tested (Fig. 3C). In contrast, the *SMF-R74A* strain was extremely sick, forming pinpoint colonies on YPD agar medium at 20°C–34°C and failing to grow at 37°C (Fig. 3C). Indeed, the SmF R74A change is the only one of the 19 single-alanine mutations in SmG, SmE, and SmF tested in this study that had an overt effect per se on yeast growth.

To probe structure–activity relations at this uniquely important side chain, we replaced Arg74 with lysine or glutamine. Whereas the *SMF-R74K* cells grew as well as wild type at all temperatures tested, the *R74Q* allele was lethal (Fig. 3C). We conclude that positive charge at position 74 is critical for yeast SmF function in vivo. Double-mutants *K32A-F33A* and *Y48A-N50A* in the SmF RNA binding sites grew well at 20°C–34°C, but formed small colonies at 37°C (Fig. 3C). The *N77A-Y80A* double mutation of the flanking subunit interfaces had no effect on growth at any temperatures tested (Fig. 3C).

Genetic interactions of Sm mutants with non-Sm splicing factors

Bridging interactions between the yeast U1 snRNP bound at the intron 5′ splice site and the Msl5•Mud2 heterodimer engaged at the intron branchpoint stabilize an early spliceosome assembly intermediate and prepare a scaffold for subsequent recruitment of the U2 snRNP to the branchpoint. Genetic analyses in yeast have revealed an extensive network of buffered functions during spliceosome assembly, defined by the numerous instances in which null alleles of vegetatively inessential splicing factors, or benign mutations in essential players, elicit synthetic lethal and sick phenotypes when combined with other benign mutations in the splicing machinery (Liao et al. 1991; Abovich et al. 1994; Colot et al. 1996; Gottschalk et al. 1998; Hausmann et al. 2008; Wilmes et al. 2008; Costanzo et al. 2010; Chang et al. 2012; Qiu et al. 2012; Schwer et al. 2013; Schwer and Shuman 2014, 2015; Jacewicz et al. 2015; Agarwal et al. 2016). The present collection of biologically active mutants targeted to conserved SmG, SmE, and SmF amino acids at their RNA binding sites or subunit interfaces enables us to survey genetic interactions of these three Sm ring subunits. To accomplish this, we constructed a series of yeast strains in which the genes encoding inessential splicing factors Mud1, Nam8, Mud2, Tgs1, Lea1, or Msl1 were deleted in the *smg*Δ p[*CEN URA3 SMG*], *sme*Δ p[*CEN URA3 SME*], and *smf*Δ p[*CEN URA3 SMF*] backgrounds, thereby allowing tests of synergy by plasmid

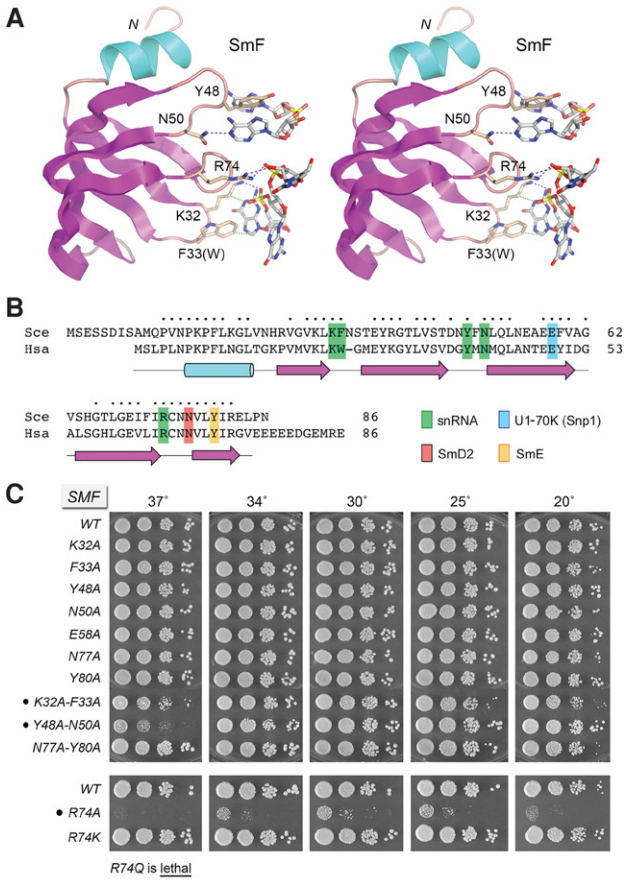

	mud1Δ	nam8Δ	mud2Δ	tgs1Δ	cbc2-Y24A	lea1Δ	msl1Δ
K32A					cs	lethal	lethal
F33A						lethal	lethal
Y48A	ts		ts	lethal		lethal	lethal
N50A						ts, cs	ts, cs
E58A	ts					ts, cs	ts, cs
R74K	ts		ts	sick	sick	lethal	lethal
N77A						sick	ts, cs
Y80A							ts
N77A-Y80A						lethal	lethal
K32A-F33A	ts	cs	cs	cs	cs		
Y48A-N50A	ts	ts	very sick	lethal	very sick		

FIGURE 3. Structure-guided mutagenesis of SmF. (*A*) Stereo view of the human U1 snRNP structure highlighting the fold of SmF (depicted as a cartoon trace with magenta β strands and a cyan α helix) and its interactions with the Sm site in U1 snRNA. Selected amino acids are shown as stick models and numbered according to their positions in the yeast SmF polypeptide. Atomic contacts are indicated by dashed lines. (*B*) Alignment of the primary structures of the *S. cerevisiae* (Sce) and human (Hsa) SmF. Positions of side chain identity/similarity are indicated by (•) *above* the yeast sequence. The secondary structure elements are depicted *below* the human sequence. SmF amino acids that make contacts to SmE, SmD2, U1 snRNP subunit Snp1/U170K or the U1 snRNA are highlighted in color-coded boxes as indicated. (*C*) Wild-type and mutated *SMF* alleles were tested for *smf*Δ complementation by plasmid shuffle. The viable FOA-resistant *smf*Δ strains bearing the indicated *SMF* alleles were spot-tested for growth on YPD agar at the temperatures specified. Alleles that conferred a conditional growth defect are denoted by (•) at *left*. (*D*) Synthetic interactions of SmF mutants. Synthetically lethal pairs of alleles are highlighted in red boxes. Other negative pairwise interactions are classified as sick or very sick (yellow boxes) or temperature-sensitive (*ts*) or cold-sensitive (*cs*) (light green boxes). Gray boxes denote lack of mutational synergy.

shuffle. Mud1 (the homolog of human U1A) and Nam8 are subunits of the yeast U1 snRNP (Gottschalk et al. 1998; Schwer et al. 2011). Mud2 (the homolog of human U2AF65) is a subunit of the Msl5•Mud2 branchpoint binding protein (Wang et al. 2008; Chang et al. 2012). Lea1 (the homolog of human U2A′) and Msl1 (the homolog of human U2B″) are subunits of the yeast U2 snRNP (Tang et al. 1996; Caspary and Séraphin 1998; Caspary et al. 1999; Schwer et al. 2011). Tgs1 is the methyltransferase enzyme that converts a 7-methylguanosine RNA cap to a 2,2,7-trimethylguanosine (TMG) cap, which is a signature modification of the U1, U2, U4, and U5 snRNAs (Mouaikel et al. 2002; Hausmann et al. 2008). In addition, we tested for genetic interactions with the cap-binding subunit of the yeast nuclear cap-binding complex (CBC). The *cbc2-Y24A* mutation in the cap-binding pocket of nuclear CBC, which has no effect per se on yeast cell growth, can either ameliorate or exacerbate the effects of mutations in other yeast splicing factors (Qiu et al. 2012).

The results of the synergy tests for *SMG*, *SME*, and *SMF* mutants are tabulated in Figures 1D, 2D, and 3D, respectively. The consistent trend for the three sets of single-alanine Sm mutations, the SmF *R74K* mutation, and the SmF *N77A-Y80A* double mutation was that the majority were lethal or growth-defective in the absence of U2 snRNP subunits Lea1 and Msl1, yet they elicited no or relatively modest synthetic phenotypes in the absence of Mud1, Nam8, Mud2, TMG caps, or when the cap-binding site of nuclear CBC was debilitated. For example, *SMG-R23A*, *SME-F49A*, *SME-K83A*, *SMF-F33A*, and *SMF-N77A-Y80A* were lethal or sick in the *lea1*Δ and *msl1*Δ backgrounds, but had no synergies with *mud1*Δ, *nam8*Δ, *mud2*Δ, *tgs1*Δ, or *cbc2-Y24A*. We surmise that the function or structural integrity of the yeast U2 snRNP is especially sensitive to otherwise benign perturbations of the RNA binding or subunit interfaces of the Sm ring when either component of the Lea1•Msl1 subassembly of the U2 snRNP is missing.

Whereas it appears that the U1 snRNP function is not as acutely sensitive to mutations of the SmG, SmE, and SmF proteins when its Mud1 or Nam8 subunits are missing, this could reflect an inherently greater level of genetic redundancy within the U1 snRNP and other components of the commitment complex (i.e., Mud2 and Cbc2). In line with the idea that the U1 snRNP function has a higher threshold for succumbing to Sm mutations, we find that a double-alanine change *F35A-N37A* of the SmG RNA binding site was lethal with *nam8*Δ, *mud2*Δ, *tgs1*Δ, and *cbc2-Y24A* and double-alanine mutation *F49A-N51A* in the SmE RNA binding site was lethal with *mud2*Δ and *tgs1*Δ (Fig. 2D). An atomic-level explanation for these synergies is elusive in the absence of a structure of the *S. cerevisiae* U1 snRNP, per se or in its interactions with Mud2•Msl5.

It is worth pointing out that the recent cryo-EM structure of a *Schizosaccharomyces pombe* spliceosome reveals that within the U2 snRNP, the Lea1•Msl1 complex packs against the SmB and SmD3 subunits of Sm, with Lea1 making direct atomic interactions with SmB (Hang et al. 2015). Thus, the synthetic lethalities of SmG, SmE, and SmF point mutations with Lea1 and Msl1 deletion are likely not explained by loss of direct physical interactions between these subcomplexes of the U2 snRNP. Previously, we had reported that single-alanine mutations in the RNA binding triad of *S. cerevisiae* SmD3 (*S39A*, *N41A*, *R65A*) and at the SmD3 interface with SmB (*K70A*) had no effect on growth per se and either no or modest (*ts*) defects in combination with *mud1*Δ, *nam8*Δ, or *mud2*Δ, but were synthetically lethal with *lea1*Δ (Schwer and Shuman 2015). Here we find that *SMD3* alleles *S39A*, *N41A*, *R65A*, and *K70A* are also lethal in the *msl1*Δ background (Supplemental Fig. S1). We extended the analysis to single-alanine mutations in the RNA binding triad of yeast SmB (*H40A, N42A, R88A*), which elicit no growth defects per se and have either no effect or a *ts* phenotype in *mud1*Δ, *nam8*Δ, or *mud2*Δ backgrounds (Schwer and Shuman 2015). The *SMB H40A, N42A,* and *R88A* alleles were uniformly lethal with *lea1*Δ and *msl1*Δ (Supplemental Fig. S1). We conclude that strong genetic interactions with Lea1•Msl1 apply to all five of the yeast Sm ring subunits that have been interrogated to date.

Effects of simultaneous mutations in Sm subunit pairs

The remarkable tolerance of the RNA binding sites of five yeast Sm proteins to single- and double-alanine mutations of the nucleotide-binding amino acids suggested that the Sm ring system has built-in redundancy, whereby the other RNA binding sites can pick up the slack when the RNA site of one subunit is mutated. This raises an important question of how many Sm RNA binding sites suffice for biological activity of the yeast Sm ring. Mutagenesis of the RNA binding triad of SmD3 (Ser-Asn-Arg) and SmB (His-Asn-Arg) provided initial insights into the redundancies of the Sm ring by showing that simultaneous alanine mutations of the Asn or Arg residues in SmD3 and SmB were lethal (Schwer and Shuman 2015). Thus, Sm ring function in vivo was fatally compromised when the sequential nucleotide-binding pockets of the SmD3 and SmB subunits lost their nucleobase hydrogen-bonding and π-cation stacking side chains.

Here we expanded the pairwise mutagenesis approach to the SmG-SmE-SmF subassembly of the yeast Sm ring. Figure 4 summarizes the effects of combining alanine mutations in the RNA binding Phe-Asn-Arg triad of SmG with alanine mutations of the RNA binding residues of SmB, SmD3, SmE, and SmF. The *SMG N37A* allele was synthetically lethal with the synonymous Asn-to-Ala alleles of *SMB* (*N42A*), *SMD3* (*N41A*), and *SME* (*N51A*) and was *ts* with the synonymous *SMF N50A* allele. *SMG N37A* was also synthetically lethal when combined with mutations of the Arg or Lys component of the RNA binding triad in all four other Sm proteins (*SMB R88A*, *SMD3 R65A*, *SME K83A*, or *SMF*

SMG vs SMB	H40A	N42A	R88A	H40A-N42A
F35A		ts		very sick
N37A	lethal	lethal	lethal	
R64A		lethal	lethal	

SMG vs SMD3	S39A	N41A	R65A	S39A-R65A	N41A-R65A
F35A					ts
N37A	very sick	lethal	lethal		
R64A		lethal	ts	lethal	

SMG vs SME	F32A	E33A	F49A	N51A	K83A	F49A-N51A
F35A						ts
N37A	ts	ts	lethal	lethal	lethal	
R64A				ts	ts	lethal

SMG vs SMF	K32A	F33A	Y48A	N50A	R74K	Y48A-N50A
F35A	ts		ts		ts	very sick
N37A	lethal	lethal	lethal	ts	lethal	
R64A	lethal		lethal		lethal	

FIGURE 4. Synergies of RNA site mutations in SmG with mutations in other Sm subunits. Synthetically lethal pairs of alleles are highlighted in red boxes. Other negative pairwise interactions are classified as sick or very sick (yellow boxes) or temperature-sensitive (*ts*) or cold-sensitive (*cs*) (light green boxes). Gray boxes denote lack of mutational synergy.

R74K) and with additional mutations in the RNA binding site of SmF (*K32A* and *F33A*). Similarly, the *SMG R64A* allele was synthetically lethal with mutations of the corresponding arginine in *SMB* (*R88A*) and *SMF* (*R74K*) and conferred a *ts* growth defect when combined with corresponding mutations in *SMD3* (*R65A*) and *SME* (*K83A*). Moreover, *SMG R64A* was lethal in combination with Asn-to-Ala changes in the triads of *SMB* (*N42A*) and *SMD3* (*N41A*) and with *SMF* alleles *K32A* and *Y48A*. In contrast, the *SMG F35A* change displayed very few synergies with other Sm RNA-site single mutations (4/16 pairwise combinations elicited a *ts* phenotype and the rest were benign). Only by combining *SMG F35A* with double-alanine RNA site mutations could a very sick phenotype be uncovered (e.g., with *SMB H40A-N42A* and *SMF Y48A-N50A*). These all-against-all results for SmG suggest that six intact RNA binding sites in the Sm ring can suffice for in vivo function, but five sites may not.

The analysis was carried forward to SmE in Figure 5, whereby we tested synergies of alanine mutations in the Phe49-Asn51-Lys83 triad and in RNA binding residues Phe32 and Glu33. On the mildest end of the spectrum, *SME E33A* had no impact in combination with single mutations of *SMB*, *SMD3*, or *SMF* (Fig. 5) and was *ts* with just one of the *SMG* alleles (*N41A*, Fig. 4). *SME E33A* did elicit nonlethal growth defects with double-mutations of *SMB* (*H40A-N42A*), *SMD3* (*N41A-R65A*), and *SMF* (*Y48A-N50A*) (Fig. 5). On the severe end of the spectrum were the *SME* triad alleles. To wit, *SME F49A* was lethal with *SMG N37A*; *SMB N42A*; *SMF* alleles *Y48A*, *R74K*, and *K32A-F33A*; and *SMD3* mutations *N41A* and *S39A-R65A* (Figs. 4, 5). *SME N51A* was lethal with *SMG N37A*; *SMD3 N41A*; and *SMF* alleles *Y48A* and *R74K*. *SME K83A* was lethal with *SMG N37A*; *SMB N42A*; *SMD3* mutations *N41A* and *S39A-R65A*; and *SMF* allele *R74K*. All three *SME* triad alleles were very sick in combination with *SMB R88A* (Fig. 5). The *SME F32A* change elicited synergies of narrower range and lesser severity; *F32A* was lethal only in combination with *SMF R74K* (Fig. 5).

Tests of *SMF* triad mutations *Y48A*, *N50A*, and *R74K* and additional RNA site mutations *K32A* and *F33A* against *SMB* and *SMD3* triad alleles (Fig. 5) completed the synthetic genetic array. *SMF* displayed a distinctive hierarchy of synergies whereby the triad asparagine mutation *N50A* was less deleterious than the triad aromatic lesion *Y48A* and the basic lesion

SME vs SMB	H40A	N42A	R88A	H40A-N42A
F32A		very sick		
E33A				very sick
F49A		lethal	very sick	
N51A		very sick	very sick	
K83A		lethal	very sick	
F49A-N51A	lethal			

SME vs SMD3	S39A	N41A	R65A	S39A-R65A	N41A-R65A
F32A		very sick			
E33A					ts
F49A		lethal		lethal	
N51A		lethal		very sick	
K83A		lethal		lethal	
F49A-N51A	very sick		very sick		

SME vs SMF	K32A	F33A	Y48A	N50A	R74K	Y48A-N50A	K32A-F33A
F32A					lethal	sick	very sick
E33A						ts	
F49A			lethal		lethal		lethal
N51A	very sick		lethal	ts	lethal		
K83A	very sick	ts	very sick		lethal		
F49A-N51A		very sick					

SMB vs SMF	K32A	F33A	Y48A	N50A	R74K	Y48A-N50A	K32A-F33A
H40A	very sick		ts		sick	very sick	lethal
N42A	lethal	lethal	lethal	ts	lethal		
R88A	lethal	very sick	lethal	ts	lethal		

SMD3 vs SMF	K32A	F33A	Y48A	N50A	R74K	K32A-F33A
S39A			ts		ts /cs	lethal
N41A	lethal	lethal	lethal	ts	lethal	
R65A	sick		lethal		lethal	
N41A-R65A				lethal		
S39A-R65A		very sick		ts		

FIGURE 5. Synergies of mutations in SmE and SmF with mutations in other Sm subunits. Synthetically lethal pairs of alleles are highlighted in red boxes. Other negative pairwise interactions are classified as sick or very sick (yellow boxes) or temperature-sensitive (*ts*) or cold-sensitive (*cs*) (light green boxes). Gray boxes denote lack of mutational synergy.

R74K. *SMF N50A* caused no worse than a *ts* growth defect in combination with several RNA site single mutations in the four other Sm subunits, and was lethal in the context of the *SMD3* double-mutation *N41A-R65A* (Figs. 4, 5). In contrast, *SMF Y48A* and *R74K* were lethal in combination with the majority of the triad mutations in all four other Sm subunits. *SMF K32A* and *F33A* also elicited synthetic lethalities with a variety of single-alanine mutations in other Sm subunits (Figs. 4, 5).

Conclusions

By leveraging snRNP structural biology and the genetics of budding yeast, we gained new insights into structure–function relationships of the essential Sm ring subunits SmG, SmE, and SmF. The results of a cumulative alanine scan of 19 conserved amino acids of these three proteins revealed that, with the exception of Arg74 in SmF, none of the residues is essential for yeast growth under standard laboratory conditions. Yet, for SmG, SmE, and SmF, as for so many components of the *S. cerevisiae* spliceosome, the effects of subtracting protein–RNA and protein–protein interactions were masked in an otherwise wild-type genetic background because of inherent functional redundancies of the yeast splicing machine. Our survey of genetic interactions with multiple non-Sm splicing factors showed that mutations of SmG, SmE, and SmF (and of SmB and SmD3) consistently elicited synthetic lethality in the absence of U2 snRNP subunits Lea1 and Msl1. Sporadic synergies of specific SmG, SmE, and SmF mutations were observed absent other early spliceosome components: Mud1, Nam8, Mud2, and TMG caps. It is possible that the hierarchy of mutational synergies skewed toward U2 snRNP reflects variations of the nucleotide sequences of the Sm sites in the *S. cerevisiae* U snRNAs. A cryo-EM model of the *S. cerevisiae* U4/U6.U5 tri-snRNP demarcates the Sm site of U4 as 5′-AAUUUUUGG and U5 as 5′-AUUUUUUGG (Wan et al. 2016). The putative Sm sites of the *S. cerevisiae* U1 and U2 snRNAs are 5′-AAUUUUU GA and 5′-AUUUUUUGG, respectively.

All-against-all pairwise combinations of SmG, SmE, SmF, SmB, and SmD3 RNA site mutations highlighted the built-in redundancies of the Sm ring, whereby subtracting RNA contacts of any one Sm subunit is tolerated but simultaneous mutations of the RNA binding sites of any two of the five Sm subunits tested can be lethal. These results suggest that six of seven intact RNA binding sites in the Sm ring can suffice for in vivo function, but five sites may not, i.e., one bad apple does not spoil the whole bunch, but two bad apples do. These conclusions apply to the five Sm subunits that have been interrogated here and previously (Schwer and Shuman 2015) by structure-guided mutagenesis and synthetic genetic array analysis. With respect to the two subunits as yet untouched, it is conceivable that the SmD1 and or SmD2 RNA binding sites are essential per se, or that yeast might survive pairwise mutations of SmD1 or SmD2 RNA sites within the ring. Thorough genetic analyses of SmD1 and SmD2 will settle the issue.

MATERIALS AND METHODS

Sm expression plasmids and mutants

A 1.19-kb DNA segment spanning the 234-bp *SMG* ORF plus 470- and 486-bp of upstream and downstream genomic sequence was PCR-amplified from *S. cerevisiae* DNA with oligonucleotide primers that introduced restriction sites for cloning into pRS316 (*CEN URA3*), pRS415 (*LEU2 CEN*), and pRS413 (*HIS3 CEN*). Missense mutations were introduced into the *SMG* gene by two-stage PCR overlap extension with mutagenic primers. The PCR products were digested and then inserted into the pRS415-SMG and pRS413-SMG expression plasmids. We used similar strategies to generate pRS316-, pRS415-, and pRS413-based expression plasmids harboring wild-type and mutated *SME* genes (spanning nucleotides −148 to +560) and *SMF* genes (nucleotides −205 to +543). All genes in the resulting plasmids were sequenced completely to confirm that no unwanted changes were acquired during amplification and cloning. We also generated pRS316-based plasmids (*URA3 CEN*) carrying pairwise combinations of *SMG* (nucleotides −470 to +720), *SME* (nucleotides −148 to +560), *SMF* (nucleotides −205 to +543), *SMB* (nucleotides −500 to +875), and *SMD3* (nucleotides −445 to +553). In the p316-SM/SM plasmids, *SMG* is arranged in a head-to-tail fashion with *SME*, *SMF*, *SMD3* or *SMB1*, while all other combinations (*SMF/SME*, *SMF/SMB*, *SMF/SMD3*, *SME/SMB*, and *SME/SMD3*) are in a head-to-head orientation.

Yeast strains and tests of function in vivo

To develop plasmid shuffle assays to test the effects of *SM* mutations in various genetic backgrounds, we first transfected heterozygous *SME sme*Δ::*kanMX*, *SMF smf*Δ::*kanMX*, and *SMG smg*Δ::*hygMX* diploids with p316-SM plasmids. The *sm*Δ [p316-SM] cells were resistant to G418 or hygromycin and unable to grow on medium containing 0.75 mg/mL 5-fluoroorotic acid (FOA). To assay the function of mutated *SM* alleles, *sm*Δ [p316-SM] cells were transfected with *CEN LEU2 SM* or *CEN HIS3 SM* plasmids. Individual Leu^+ or His^+ transformants were selected and streaked on agar medium containing FOA. The plates were incubated at 20, 30, or 37°C and mutants that failed to form macroscopic colonies at any temperature after 8 d were deemed lethal. Individual FOA-resistant colonies with viable *SM* alleles were grown to mid-log phase in YPD broth and adjusted to the same A_{600} values. Aliquots (3 µL) of serial 10-fold dilutions were spotted to YPD agar plates, which were then incubated at temperatures ranging from 18°C or 20°C to 37°C. We also developed plasmid shuffle assays to test the effects of *SMG*, *SME*, and *SMF* mutations in *nam8*Δ, *mud1*Δ, *mud2*Δ, *tgs1*Δ, *cbc2-Y24A*, *lea1*Δ, and *msl1*Δ genetic backgrounds, using standard genetic manipulations of mating, sporulation, and dissection.

Tests of mutational synergy with other Sm subunits

Nine haploid strains in which pairs of *sm*Δ alleles are complemented by the corresponding p316-SM/SM plasmids were generated by pairwise crossing of *sm*Δ p316-SM haploids of the opposite mating

type. The heterozygous diploids were plated to 5-FOA agar to select against the *URA3 CEN SM* plasmids and subsequently transfected with the appropriate p316-SM/SM plasmids. Ura$^+$ transformants were selected and subjected to sporulation and dissection. The strains and plasmids for *SMB* and *SMD3* genetics were described previously (Schwer and Shuman 2015). We thereby generated strains *smgΔ::hygMX smeΔ::kanMX* p[*URA3 CEN SMG SME*], *smgΔ::hygMX smfΔ::kanMX* p[*URA3 CEN SMG SMF*], *smgΔ::hygMX smbΔ::kanMX* p[*URA3 CEN SMG SMB*], *smgΔ::hygMX smd3Δ::hygMX* p[*URA3 CEN SMG SMD3*], *smfΔ::kanMX smeΔ::natMX* p[*URA3 CEN SMF SME*], *smfΔ::kanMX smbΔ::natMX* p[*URA3 CEN SMF SMB*], *smfΔ::kanMX smd3Δ::hygMX* p[*URA3 CEN SMF SMD3*], *smeΔ::kanMX smbΔ::natMX* p[*URA3 CEN SME SMB*], *smeΔ::kanMX smd3Δ::hygMX* p[*URA3 CEN SME SMD3*] that failed to grow on 5-FOA medium unless they had been co-transformed with *CEN HIS3* plus *CEN LEU2* plasmids harboring the corresponding *SM* genes. The function of mutated *SM* alleles in various combinations was assessed as described above.

SUPPLEMENTAL MATERIAL

Supplemental material is available for this article.

ACKNOWLEDGMENTS

This work was supported by National Institute of General Medical Sciences (NIGMS, NIH) grants GM52470 (S.S. and B.S.) and GM102961 (B.S.).

Received May 10, 2016; accepted June 14, 2016.

REFERENCES

Abovich N, Liao XC, Rosbash M. 1994. The yeast MUD2 protein: an interaction with PRP11 defines a bridge between commitment complexes and U2 snRNP addition. *Genes Dev* **8:** 843–854.

Agarwal R, Schwer B, Shuman S. 2016. Structure–function analysis and genetic interactions of the Luc7 subunit of the *Saccharomyces cerevisiae* U1 snRNP. *RNA* (this issue). doi: 10.1261/rna.056911.116.

Bordonné R. 2000. Functional characterization of nuclear localization signals in yeast Sm proteins. *Mol Cell Biol* **20:** 7943–7954.

Caspary F, Séraphin B. 1998. The yeast U2A′/U2B complex is required for pre-spliceosome formation. *EMBO J* **17:** 6348–6358.

Caspary F, Shevchenko A, Wilm M, Séraphin B. 1999. Partial purification of the yeast U2 snRNP reveals novel yeast pre-mRNA splicing factor required for pre-spliceosome assembly. *EMBO J* **18:** 3463–3474.

Chang J, Schwer B, Shuman S. 2012. Structure-function analysis and genetic interactions of the yeast branchpoint binding protein Msl5. *Nucleic Acids Res* **40:** 4539–4552.

Chari A, Paknia E, Fischer U. 2009. The role of RNP biogenesis in spinal muscular atrophy. *Curr Opin Cell Biol* **21:** 387–393.

Colot HV, Stutz F, Rosbash M. 1996. The yeast splicing factor Mud13p is a commitment complex component and corresponds to CBP20, the small subunit of the nuclear cap-binding complex. *Genes Dev* **10:** 1699–1708.

Costanzo M, Baryshnikova A, Bellay J, Kim Y, Spear ED, Sevier CS, Ding H, Koh JL, Toufighi K, Mostafavi S, et al. 2010. The genetic landscape of a cell. *Science* **327:** 425–431.

Gottschalk A, Tang J, Puig O, Salgado J, Neubauer G, Colot HV, Mann M, Séraphin B, Rosbash M, Lührmann R, et al. 1998. A comprehensive biochemical and genetic analysis of the yeast U1 snRNP reveals five novel proteins. *RNA* **4:** 374–393.

Grimm C, Chari A, Pelz JP, Kuper J, Kisker C, Diederichs K, Stark H, Schindelin H, Fischer U. 2013. Structural basis of assembly chaperon-mediated snRNP formation. *Mol Cell* **49:** 692–703.

Hang J, Wan R, Yan C, Shi Y. 2015. Structural basis of pre-mRNA splicing. *Science* **349:** 1191–1198.

Hausmann S, Zheng S, Costanzo M, Brost RL, Garcin D, Boone C, Shuman S, Schwer B. 2008. Genetic and biochemical analysis of yeast and human cap trimethylguanosine synthase: functional overlap of TMG caps, snRNP components, pre-mRNA splicing factors, and RNA decay pathways. *J Biol Chem* **283:** 31706–31718.

Jacewicz A, Chico L, Smith P, Schwer B, Shuman S. 2015. Structural basis for recognition of intron branchpoint RNA by yeast Msl5 and selective effects of interfacial mutations on splicing of yeast pre-mRNAs. *RNA* **21:** 401–414.

Kambach C, Walke S, Yound R, Avis JM, de la Fortelle E, Raker VA, Lührmann R, Li J, Nagai K. 1999. Crystal structures of two Sm protein complexes and their implications for the assembly of the spliceosomal snRNPs. *Cell* **96:** 375–387.

Kondo Y, Oubridge C, van Roon AM, Nagai K. 2015. Crystal structure of human U1 snRNP, a small nuclear ribonucleoprotein particle, reveals the mechanism of 5′ splice site recognition. *eLife* **4:** e04986.

Kroiss M, Schultz J, Wiesner J, Chari A, Sickmann A, Fischer U. 2008. Evolution of an RNA assembly system: a minimal SMN complex facilitates formation of UsnRNPs in *Drosophila melanogaster*. *Proc Natl Acad Sci* **105:** 10045–10050.

Li J, Leung AK, Kondo Y, Oubridge C, Nagai K. 2016. Re-refinement of the spliceosomal U4 snRNP core-domain structure. *Acta Crystallogr D Struct Biol* **72:** 131–146.

Liao XC, Tang J, Rosbash M. 1991. An enhancer screen identifies a gene that encodes the yeast U1 snRNP A protein: implications for snRNP protein function in pre-mRNA splicing. *Genes Dev* **7:** 419–428.

Liu Q, Fischer U, Wang F, Dreyfuss G. 1997. The spinal muscular atrophy gene product, SMN, and its associated protein SIP1 are in a complex with spliceosomal snRNP proteins. *Cell* **90:** 1013–1021.

Lunn MR, Wang CH. 2008. Spinal muscular atrophy. *Lancet* **371:** 2120–2133.

Mouaikel J, Verheggen C, Bertrand E, Tazi J, Bordonné R. 2002. Hypermethylation of the cap structure of both yeast snRNAs and snoRNAs requires a conserved methyltransferase that is localized to the nucleolus. *Mol Cell* **9:** 891–901.

Neuenkirchen N, Englbrecht C, Ohmer J, Ziegenhals T, Chari A, Fischer U. 2015. Reconstitution of the human U snRNP assembly machinery reveals stepwise Sm protein organization. *EMBO J* **34:** 1925–1941.

Nguyen THD, Galej WP, Bai X, Savva CG, Newman AJ, Scheres SHW, Nagai K. 2015. The architecture of the spliceosomal U4/U6.U5 tri-snRNP. *Nature* **523:** 47–52.

Noble SM, Guthrie C. 1996. Transcriptional pulse-chase analysis reveals a role for a novel snRNP-associated protein in the manufacture of spliceosomal snRNPs. *EMBO J* **15:** 4368–4379.

Qiu ZR, Chico L, Chang J, Shuman S, Schwer B. 2012. Genetic interactions of hypomorphic mutations in the m^{7}G cap binding pocket of yeast nuclear cap binding complex: an essential role for Cbc2 in meiosis via splicing of *MER3* pre-mRNA. *RNA* **18:** 1996–2011.

Schwer B, Shuman S. 2014. Structure-function analysis of the Yhc1 subunit of yeast U1 snRNP and genetic interactions of Yhc1 with Mud2, Nam8, Mud1, Tgs1, U1 snRNA, SmD3 and Prp28. *Nucleic Acids Res* **42:** 4697–4711.

Schwer B, Shuman S. 2015. Structure-function analysis and genetic interactions of the Yhc1, SmD3, SmB, and Snp1 subunits of yeast U1 snRNP and genetic interactions of SmD3 with U2 snRNP subunit Lea1. *RNA* **21:** 1173–1186.

Schwer B, Erdjument-Bromage H, Shuman S. 2011. Composition of yeast snRNPs and snoRNPs in the absence of trimethylguanosine caps reveals nuclear cap binding protein as a gained U1 component implicated in the cold-sensitivity of *tgs1Δ* cells. *Nucleic Acids Res* **39:** 6715–6728.

Schwer B, Chang J, Shuman S. 2013. Structure-function analysis of the 5′ end of yeast U1 snRNA highlights genetic interactions with the

Msl5•Mud2 branchpoint binding complex and other spliceosome assembly factors. *Nucleic Acids Res* **41:** 7485–7500.

Tang J, Abovich N, Rosbash M. 1996. Identification and characterization of a yeast gene encoding the U2 small ribonucleoprotein particle B″ protein. *Mol Cell Biol* **16:** 2787–2795.

van der Feltz C, Anthony K, Brilot A, Pomeranz Krummel DA. 2012. Architecture of the spliceosome. *Biochemistry* **51:** 3321–3333.

Wan R, Yan C, Bai R, Wang L, Huang M, Wong C, Shi Y. 2016. The 3.8 Å structure of the U4/U6.U5 tri-snRNP: insights into spliceosome assembly and catalysis. *Science* **351:** 466–475.

Wang Q, Zhang L, Lynn B, Rymond BC. 2008. A BBP–Mud2p heterodimer mediates branchpoint recognition and influences splicing substrate abundance in budding yeast. *Nucleic Acids Res* **36:** 2787–2798.

Weber G, Trowitzsch S, Kastner B, Lührmann R, Wahl MC. 2010. Functional organization of the Sm core in the crystal structure of human U1 snRNP. *EMBO J* **29:** 4172–4184.

Wilmes GM, Bergkessel M, Bandyopadhyay S, Shales M, Braberg H, Cagney G, Collins SR, Whitworth GB, Kress TL, Weissman JS, et al. 2008. A genetic interaction map of RNA-processing factors reveals links between Sem1/Dss1-containing complexes and mRNA export and splicing. *Mol Cell* **32:** 735–746.

Zhang D, Abovich N, Rosbash M. 2001. A biochemical function for the Sm complex. *Mol Cell* **7:** 319–329.

Zhang R, So BR, Li P, Yong J, Glisovic T, Wan L, Dreyfuss G. 2011. Structure of a key intermediate of the SMN complex reveals Gemin2's crucial function in snRNP assembly. *Cell* **146:** 384–395.